

Electrochemical Corrosion Performance of FSSP-Modified Copper Alloy Surface

Wei-wei Song^{1,2,3,*}, Dun-wen Zuo², Xiao-jing Xu³, Hong-feng Wang¹, Sheng-rong Liu¹

¹ College of Mechanical and Electrical Engineering, Huangshan University, Huangshan 245041, P. R. China

² College of Mechanical and Electrical Engineering, Nanjing University of Aeronautics and Astronautics, Nanjing 210016, P. R. China

³ School of Mechanical Engineering, Jiangsu University, Zhenjiang 212013, P. R. China

*E-mail: sww_2011@163.com

Received: 4 April 2019 / Accepted: 4 June 2019 / Published: 30 June 2019

This study proposed a method using the friction stir surface processing (FSSP) technology to modify the surface layer of copper alloy and hence improve its corrosion resistance. H62 copper alloy was used for the purpose. The modification parameters in the FSSP were set as follows: rotation speed, 1200 rpm; traversing speed, 150 mm/min; and depth 0.15 mm. The findings revealed that the surface of the modified sample with a depth of 0.15 mm had a higher degree of metallographic refinement and better hardness and corrosion resistance. The modified samples after one, two and three passes were compared. It was found that the metallographic structure of the two-pass modified samples was fine and uniform, and the hardness and corrosion resistance were the best, followed by the one-pass modification, with the three-pass modification being the worst.

Keywords: Electrochemical corrosion; friction stir surface processing; FSSP; H62 copper alloy; modified surface; weight loss

1. INTRODUCTION

Copper alloys are widely used in aerospace, marine, high-speed trains, automotive, electronics and many other industrial fields due to their good thermal and electrical conductivity [1-8]. In some harsh environments, such as ship propellers, gear pumps for waste liquids and so on, copper alloys usually fail due to their poor corrosion resistance [9-12]. Therefore, improving the corrosion resistance of the surface layer of copper alloy has become a research hotspot. Metikoš-Huković [13] analyzed the effect of nickel content in copper alloy on the corrosion resistance of the alloy. They obtained the best nickel content for the formation of oxide film in the corrosion process, thereby improving the

corrosion resistance of the copper alloy. Rajasekaran [14] analyzed the effect of copper–nickel alloy on the corrosion resistance by plating a layer of nickel on the surface of copper alloy. Nikolaychuk [15] used the displacement solution model to study the effects of the thermodynamic properties of copper–nickel solid solutes on the corrosion–electrochemical behavior of copper–nickel alloys. Mahmoud [16] studied the corrosion of copper–iron alloy in the sodium chloride brine. Under certain pitting potentials, copper and iron were pitted, and the addition of inorganic additives inhibited the pitting corrosion. Related studies also suggested that adding some elements to the copper alloy could improve its corrosion resistance. In summary, all methods for improving the corrosion resistance of copper alloys were chemical methods. These methods were complicated in operation and high in pollution, and hence it was difficult to maintain green environmental protection processing [17–20]. From the environmental protection point of view, this study proposed a method using the friction stir surface processing (FSSP) technology to modify the surface layer of copper alloy and hence improve its corrosion resistance. This method was simple, and the surface layer of the copper alloy was rubbed using the tool without a pin to realize surface modification. The influence of surface depth (the depth of the tool) and different passes (the number of times the tool was squeezed at the same position) of FSSP on the corrosion resistance of copper alloy was analyzed, providing theoretical guidance for practical engineering application.

2. EXPERIMENT

2.1 Experimental materials

This study used the hot rolled H62 copper alloy plate. The main chemical composition is shown in Table 1, and the size of the plate used for the experiment was $200 \times 200 \times 10$ (mm).

Table 1. Chemical compositions of H62 copper alloy (mass fraction, %)

Cu	Fe	Pb	Ni	Zn	Impurities
60.5–63.5	0.15	0.08	0.5	Balance	0.3

2.2 Experimental equipment and method

The equipment used in the FSSP experiment was the FSW-LS-A10-type friction stir processing equipment (AVIC Beijing Saifusite Technology Co., Ltd, China). The FSSP tool is a needleless tool with a diameter of 20 mm.

The process parameters used in the FSSP were as follows: rotation speed of 1200 rpm and traversing speed of 150 mm/min. The number, parameters and process description of each sample is shown in Table 2.

Table 2. Number, parameters and process description of each sample

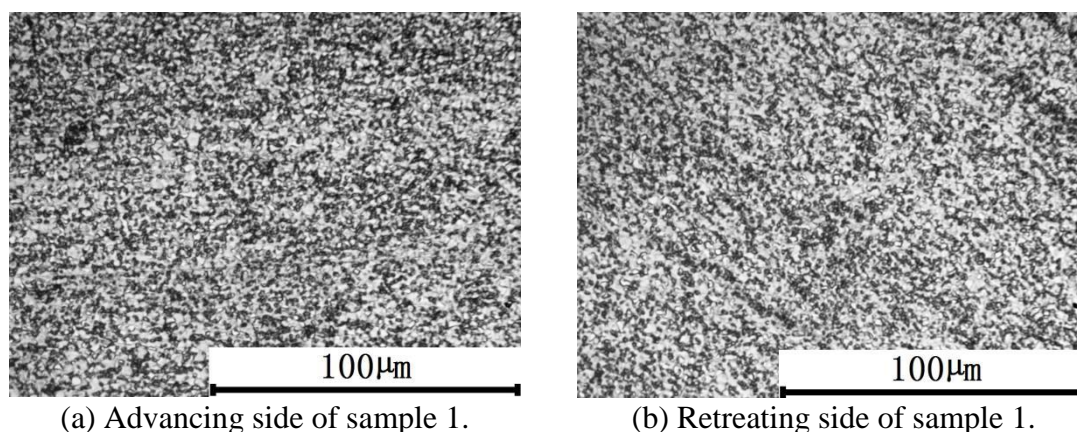
Sample number	FSSP parameters	Process description
1		Depth $\Delta = 0.15$ mm
2	Rotation speed: 1200 rpm, Traversing speed: 150 mm/min	First depth $\Delta = 0.15$ mm Second depth $\Delta = 0.15$ mm
3		First depth $\Delta = 0.15$ mm Second depth $\Delta = 0.15$ mm Third depth $\Delta = 0.15$ mm

The metallographic structure of the modified H62 copper alloy layer was analyzed using an MDS400 inverted metallographic microscope (Chongqing Aote Optical Instrument Co., Ltd, China). The hardness of the modified layer was measured using the Rockwell hardness tester of HRS-150 (Jinan Hengxu Testing Machine Technology Co., Ltd, China). A ball indenter of diameter 1.5875 mm was used in the experiment. The initial, main, and total test forces used were 10, 90, 100 kg, respectively, and the loading and unloading time was 10 s. Each test point was centered on it. Three nearby point tests were selected, and the average was taken as the hardness value of this point. Electrochemical corrosion was applied using the CS series electrochemical workstation (Wuhan Kesite Instrument Co., Ltd, China). The electrochemical solution used was 3.5% NaCl. The electrochemical corrosion experiment was carried out at room temperature. Dynamic potential scanning was used for the corrosion process, with a scanning range of -0.2 – 0.2 V, rate of 0.5 mV/s, frequency of 2.00 Hz, duration of 800 s, and open circuit potential of -0.26853 V. The photographs were taken using a scanning electron microscope (SEM) with an EDAX spectrometer (Hitachi, Ltd, Japan; model S3400).

3. RESULTS AND DISCUSSION

3.1 Metallographic analysis

Figure 1 shows the metallographic structure of the surface of the FSSP-modified copper alloy under different passes at a rotation speed of 1200 rpm, traversing speed of 150 mm/min, and depth of 0.15 mm.



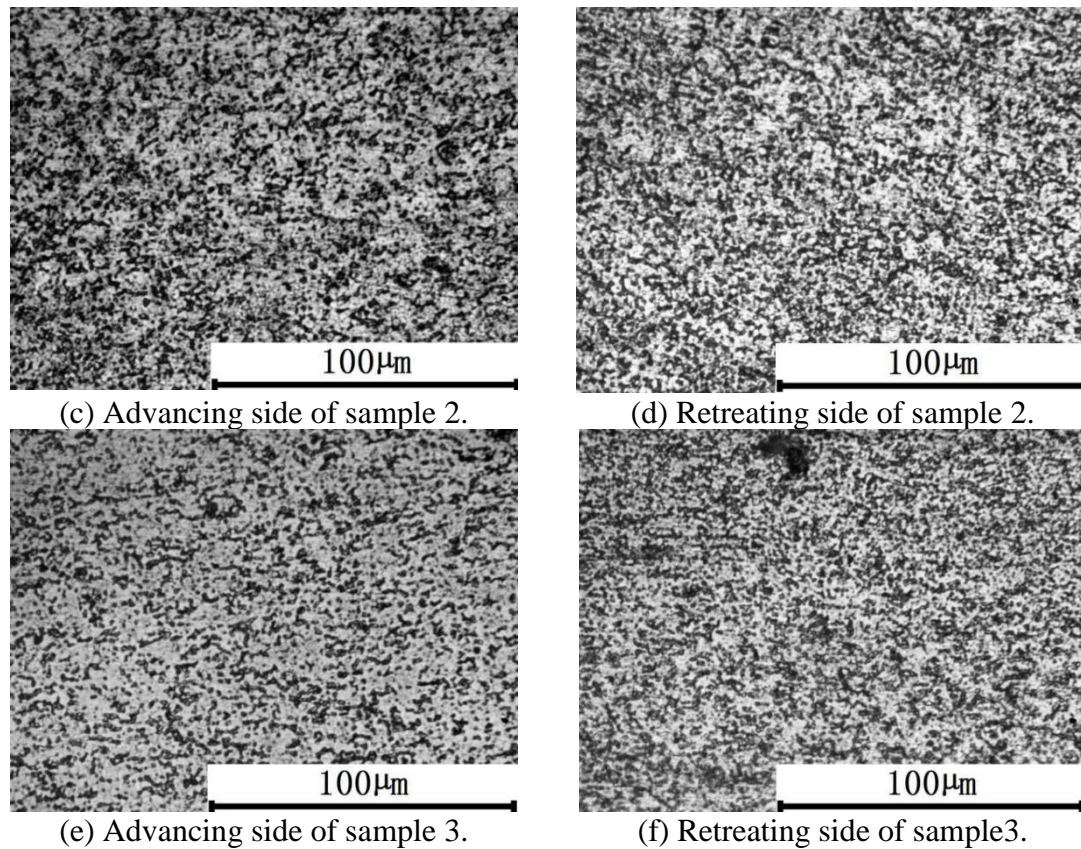


Figure 1. Metallographic structures of advancing side and retreating side of each sample (Process parameters of each pass: $\omega = 1200$ rpm, $v = 150$ mm/min, and $\Delta = 0.15$ mm. Sample1: one-pass, Sample2: two-pass, Sample3: three-pass)

Figure 1 shows that when the FSSP parameters were the same, the modified surface grains obtained by the different pass modification processes were fine and the microstructures were uniform, and no obvious holes, pores, inclusions and other defects. This is mainly due to the adoption of FSSP modification method, which further promoted the internal plastic flow and uniform distribution of the plastic metal, and broken the coarse grain, so as to obtain the modified surface copper alloy structure refinement and uniform distribution. The above explanation is consistent with literature [21-22]. Moreover, as the number of passes increased, the degree of grain refinement of the modified surface layer increased first and then decreased. The main reason for this phenomenon was that during the one-pass modification process, FSSP can promote the plastic flow of surface metal in the modified area by selecting appropriate process parameters, but the short modification time of one-pass FSSP cannot guarantee sufficient dynamic recrystallization of the structure in the modified area, so the phenomenon of uneven grain refinement occurs, which is consistent with the explanation in literature [23-24]. In the two-pass modification process, the grain refinement degree was the most obvious, indicating that the dynamic recrystallization of surface microstructure in the modified area was fully carried out, which is consistent with the explanation in literature [25]. The activation energy of grain growth and the growth index of grain growth reflect the difficulty of starting grain growth and the size of grain growth rate from the perspective of thermodynamics and kinetics. When in the two-pass processing, the temperature can ensure that the refined grain is in a stable state, and the grain is not easy to grow. At

the three-pass modification process stage, due to the higher friction heat, the grain growth index decreased, the grain boundary migration resistance decreased, but the grain grew. In the process of FSSP modified copper alloy, the increase of growth activation energy is mainly affected by the strong texture of fine crystal structure. High texture strength means that the orientation difference between grains is small and the grain boundary energy is low. This analysis is consistent with literature [26]. Figure 1 also shows that the part of the grain on the advancing side of each sample was still slightly larger than that on the retreating side. This is because the heat on the advancing side is higher than that on the retreating side. Under the same condition, high heat is prone to part of the grain growth, which is consistent with the analysis in literature [27].

Figure 2 shows the metallographic structure of the H62 copper alloy. The grain was strip-shaped because the base material was a rolled sheet.

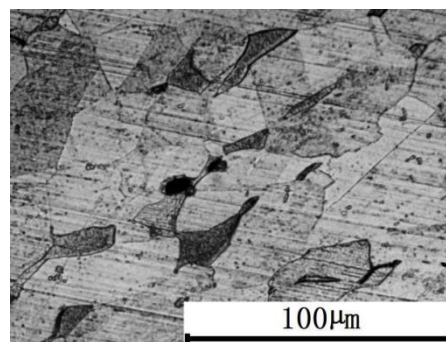


Figure 2. Metallographic structure of the base metal.

3.2 Hardness analysis

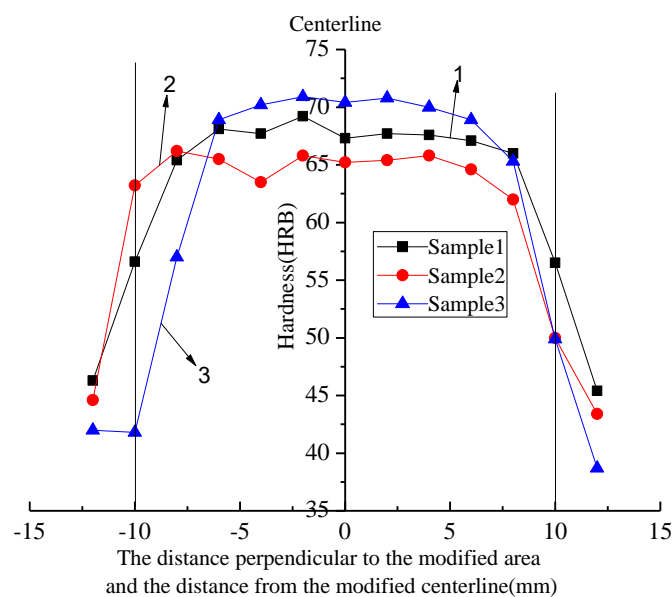


Figure 3. Hardness curves of modified surfaces of each sample. (Process parameters of each pass: $\omega = 1200$ rpm, $v = 150$ mm/min, and $\Delta = 0.15$ mm. Sample1: one-pass, Sample2: two-pass, Sample3: three-pass)

Figure 3 shows the hardness values of the modified layers of different samples perpendicular to the modified zone. Central area of copper alloy under the effect of the tool, the frictional heat generated in the region try to recrystallization occur, formed the tiny recrystallization grain size, the unit volume increase in the number of grain boundary and grain boundary can effectively prevent the dislocation glide, improve the creep resistance of copper alloy material, so as to improve the hardness of copper alloy. This is consistent with literature [28] analysis. As can be seen from figure 5, with the increase of modified passes, the hardness fluctuation degree of the modified area decreases, indicating that the homogeneity of the structure in the modified area increases. This analysis is consistent with literature [25]. The figure 5 clearly shows that the hardness distribution of each sample was relatively uniform, that is, the hardness values of the advancing and retreating sides were substantially symmetrical, and the hardness value of the advancing side phase in the center of the modified region was slightly lower compared with that on the retreating side. This is consistent with literature [23]. FSSP modified surface hardness is higher than the base, and the hardness of the friction stir welding area is lower than the parent metal, this is because the friction stir welding area precipitation secondary relative to the influence of the welding zone hardness than the grain size of the welding area, the influence of hardness and FSSP modified surface layer of metal does not appear the second phase, which is consistent with the literature[29-30]. The average hardness of samples 1–3 was higher than the hardness of the base material (55.3 HRB), which was 62.38 HRB, 60.40 HRB and 60.37 HRB, respectively. The hardness values in Figure 3 were basically consistent with those obtained by metallographic structure analysis in Figures 1.

3.3 Electrochemical corrosion performance analysis

3.3.1 Corrosion weight analysis

Table 3 lists the difference in weights before and after electrochemical corrosion testing of each sample.

Table 3. Weight before and after electrochemical corrosion of each sample and base metal (Process parameters of each pass: $\omega = 1200$ rpm, $v = 150$ mm/min, and $\Delta = 0.15$ mm. Sample1: one-pass, Sample2: two-pass, Sample3: three-pass)

Sample number	Weight before experiment (g)	Weight after experiment (g)	Weight difference (g)
1	26.620	26.618	0.002
2	25.320	25.319	0.001
3	26.619	26.494	0.125
Base metal	25.418	24.435	0.983

Table 3 shows that at the rotation speed of 1200 rpm and traversing speed of 150 mm/min, the weight loss of the surface of the copper alloy obtained by the one-pass FSSP at depths 0.15mm was

0.002g. This was basically the same as that obtained by metallographic structure analysis in Figure 1. The metallographic structure obtained in sample 1 was uniformly refined, and therefore its corrosion resistance was good. Table 3 shows that when the rotation speed was 1200 rpm, traversing speed was 150 mm/min, and depth was 0.15 mm, the surface layers of copper alloy were modified using one-, two-, and three-pass FSSP, respectively. The corresponding weight loss after electrochemical corrosion was 0.002, 0.001, and 0.125 g, respectively. This was consistent with that obtained by the metallographic structure analysis in Figure1. The crystal grains of sample 2 were the finest and uniform, and therefore its corrosion resistance was the best, followed by sample 1, and finally sample 3. All samples had less corrosion loss than the base metal. The results in Table 3 were basically consistent with those of the hardness analysis in Figure 3, except that the hardness of sample 2 was slightly lower than that of sample 1, which was related to the test method, equipment and grain heterogeneity after modification. However, the general trend was basically the same.

3.3.2 Corrosion polarization curve analysis

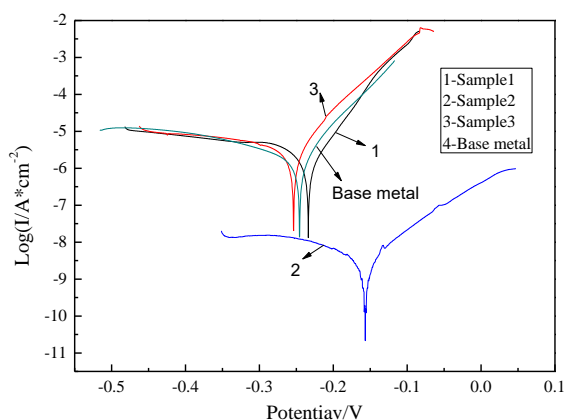


Figure 4. Electrochemical corrosion polarization curves of each sample and base metal ($\omega = 1200$ rpm, $v = 150$ mm/min, and $\Delta = 0.15$ mm. Sample1: one-pass, Sample2: two-pass, Sample3: three-pass)

Table 4. The corrosion potential and corrosion current of each sample and base metal ($\omega = 1200$ rpm, $v = 150$ mm/min, and $\Delta = 0.15$ mm. Sample1: one-pass, Sample2: two-pass, Sample3: three-pass)

Sample number	Corrosion potential (V)	Corrosion current (A/cm ²)
1	-0.234	1.86e-5
2	-0.157	7.14e-9
3	-0.254	1.03e-5
Base metal	-0.246	1.97e-4

Figure 4 shows the electrochemical corrosion polarization curves of different samples. Figure 4 shows the corrosion potential and corrosion current of each sample and base metal. Material has good corrosion resistance when the corrosion potential is big and corrosion current is small[31]. At the same time, according to literature [32], it is known that the higher the corrosion potential is, the higher the breakdown potential required for material pitting corrosion is not easy to be eroded in the natural state, the better the corrosion resistance of the material measured. In the electrochemical corrosion process of each sample, because of the negative potential of zinc, zinc is preferentially dissolved in the corrosion environment, resulting in zinc removal corrosion. However, with the increase of corrosion potential, all samples show passivation. According to the selective dissolution process of zinc, zinc dissolution is selected first, and then copper dissolution occurs, i.e



Since the experiment was carried out in a sealed container, it did not happen



Therefore, passivation will not occur in the electrochemical corrosion process of each sample[33].

In combination with Table 3, this figure clearly shows that the corrosion potential of sample 2 was the highest and the corrosion current was the smallest. Therefore, the corrosion resistance of sample 2 was the best, followed by sample 1. The corrosion potential of sample 1 was less than that of sample 3. The corrosion current of sample 1 was much smaller than that of sample 3, so its corrosivity was second only to sample 2. Figure 4 shows that the electrochemical corrosion of each sample was less passivated, and sample 1 might have a certain degree of passivation and form a passivation film to protect itself from being continuously corroded, which is why the total amount of corrosion was small. Almost no passivation marks were observed on the remaining samples. The corrosion resistance of sample 2 and 1 was significantly higher than that of the base metal, and the corrosion resistance of sample 3 was slightly different from that of the base metal. At the same time, the results of Figure 4 were basically consistent with the previous metallographic structure and hardness analysis, indicating that the electrochemical corrosion performance of the sample was inseparable from its metallographic structure and hardness.

3.3.3 SEM analysis of corrosion surface

Figure 5 shows the SEM photographs of electrochemical corrosion of different samples and base metal. The traces of the friction stir extrusion could be clearly seen from the figure. In particular, samples 1, 2 and 3 were more conspicuous.

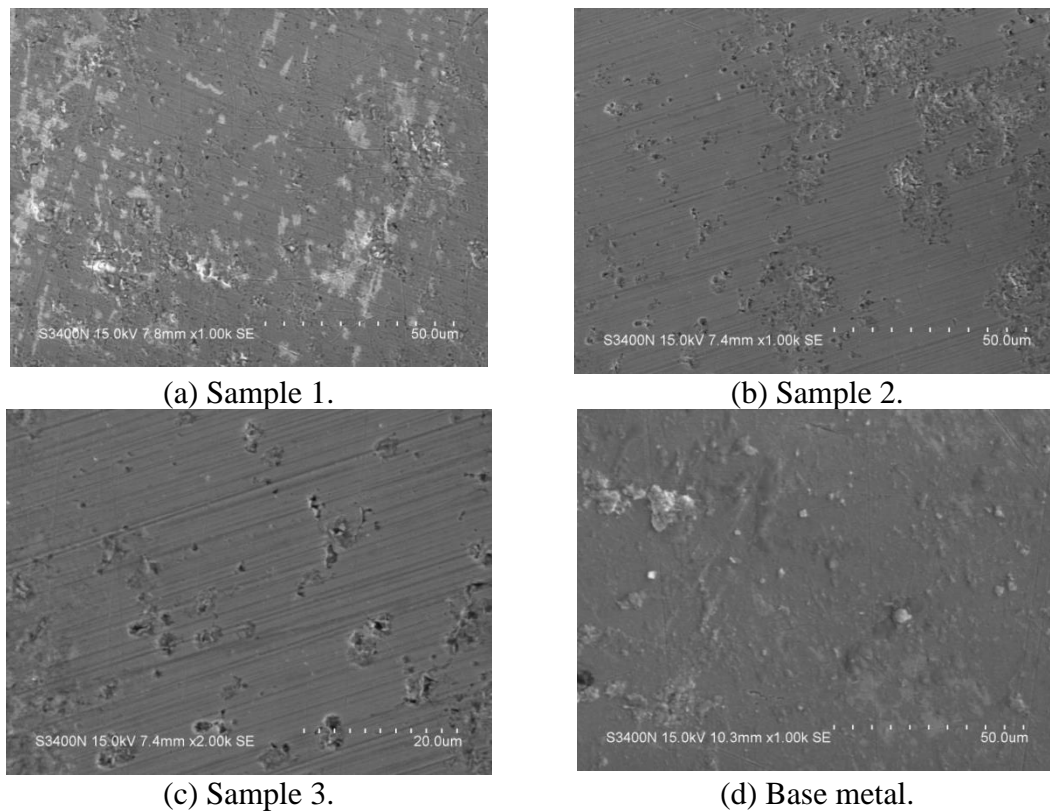


Figure 5. SEM photographs of electrochemical corrosion of each sample and base metal ($\omega = 1200$ rpm, $v = 150$ mm/min, and $\Delta = 0.15$ mm. Sample1: one-pass, Sample2: two-pass, Sample3: three-pass)

Figure 5a, 5b and 5c shows, respectively, that sample 2 had fewer pits and less pit density; sample 3 had a large corrosion pit; and although the corrosion pit of sample 1 was small, the whole sample was distributed, and severe corrosion occurred in some places. Based on the aforementioned comparison, the degree of corrosion of sample 2 was relatively small, so sample 2 was corrosion resistant. Figure 5d shows the SEM photograph of the base material after corrosion. Although the extrusion marks of the base material could not be seen from the figure, the corrosion characteristics of the base material surface were still obvious, especially the appearance of corrosion peeling layer and spot peeling. It was further explained that the corrosion resistance of the base material was not as good as that of the FSSP-modified copper alloy. This was basically consistent with Figure 5 and the previous metallographic structure and hardness analysis. This further demonstrated that sample 2 had the best corrosion resistance. As described in the literature^[34-35], from the perspective of corrosion science, chemical composition homogenization can reduce the tendency of materials to form locally corroded galvanic cells, thus contributing to the improvement of corrosion resistance of materials.

3. CONCLUSIONS

(1) When the rotation speed was 1200 rpm, forward speed was 150 mm/min, and pressing amount was 0.15 mm, one-, two- and three-pass FSSP techniques were performed for the modification.

The surface metallographic structure obtained by the two-pass modification was the finest and evenly distributed. The grains of all the modified copper alloy surface layers were finer than the base material.

(2) The average hardness of each modified sample was small, wherein the average hardness of samples 1, 2 and 3 was 62.38HRB, 60.40 HRB and 60.37 HRB, respectively, which was higher than that of the base metal (55.3 HRB). The highest was 12.8% higher than the base metal, and the lowest was 9.2% higher than the base metal.

(3) When the rotation speed was 1200 rpm, forward speed was 150 mm/min, and pressing amount was 0.15 mm, the corrosion resistance of the surface of the two-pass modified copper alloy was the best, followed by that of the one-pass modified copper alloy surface layer, and the worst was that of the three-pass modified copper alloy surface layer. However, all samples had better corrosion resistance compared with the base metal.

ACKNOWLEDGMENTS

Financial support for this study was provided by the Key Research and Development Project from Anhui Province of China (Grant No. 1704a0902053); the Key Natural Science Foundation of Anhui Higher Education Institutions of China (Grant No. KJ2016A681); the Major Natural Science Foundation of Anhui Higher Education Institutions of China (Grant No. KJ2016SD55); the Open Research Project of Anhui Simulation Design and Modern Manufacture Engineering Technology Research Center (Huangshan University; Grant No. SGCZXZD03); and the Huangshan University Talent Start Project (Grant No. 2018xkjg006).

References

1. S. Rathee, S. Maheshwari, A. N. Siddiquee and M. Srivastava, *Defence Tech.*, 13(2017) 86.
2. H. G. Rana, V. J. Badheka and A. Kumar, *Procedia Tech.*, 23 (2016) 519.
3. V. P. Vivek, J. B. Vishvesh and K. Abhishek, *Procedia Tech.*, 23 (2016) 537.
4. S. J. Abraham, S. C. R. Madane, I. Dinaharan and L. J. Baruch, *J. As. Cer. S.*, 4(2016) 381.
5. W. W. Song, X. J. Xu, D. W. Zuo and J. L. Wang, *Anti-Corros. Methed M.*, 63 (2016) 190.
6. I. Dinaharan, N. Murugan and A. Thangarasu, *J. E. S.Tech.*, 19 (2016) 1132.
7. W. W. Song, X. J. Xu, D. W. Zuo, J. L. Wang and G. Wang, *Mater. Sci-Medzg.*, 23 (2017) 222.
8. Y. T. Zhao, X. Z. Kai, G. Chen, W. L. Lin and C. M. Wang, *Prog. Nat. Sci-Mater.*, 26 (2016) 69.
9. W. L. Wang, W. Wang, W. Guo, *Hot Wor. Tech.*, 38(2009)8.
10. Y.F. Gao, Y. Yu, Y.F. Guo, W.J. Mei, P. Jiang and Z.Y. Liu, *Welding Tech.*, 47(2018)78.
11. X.J. Wang, H.W. Zhang, Z.K. Zhang and D.B. Han, *Welding*, 1(2009)25.
12. J.M. Zhao, S.Y. Gao, M.Q. Mu, R.D. Fu and Y.J. Li, *Chin. J. Lasers*, 43(2016)0106003-1.
13. M. Metikoš-Huković, I. Škugor, Z. Grubač and R. Babić, *Electrochimica Acta*, 55(2010)3123.
14. N. Rajasekaran and S. Mohan, *J. Appl. Electrochem.*, 39(2009)1911.
15. P.A. Nikolaychuk and A.G. Tyurin, *Physicochem. Problems Mater. Protection*, 48(2012)462.
16. S.S. Mahmoud, *J. Alloys Compd.*, 457(2008)587.
17. K. Siegert and S. Huber, *Mater. Sci. Eng. A.*, 326 (2002) 63.
18. S. Dai, D. W. Zuo, C. Fang, L. Zhu, H. Cheng, Y. X. Gao and W. W. Li, *Mater. Trans.*, 57 (2016) 539.
19. J. S. Kim, Y. S. Kwon, O. I. Lomovsky, D. V. Dudina, V. F. Kosarev, S. V. Klinkov, D. H. Kwon and I. Smurov, *Compos. Sci. Tech.*, 67 (2007) 2292.
20. H.F. Wang, J. L. Wang, W. W. Song, D.W. Zuo and D.L. Shao, *Int. J. Electrochem. Sci.*, 11(2016) 6933.

21. Y. Z. Li and J. Kong, *Hot Wor. Tech.*, 46(2017)82.
22. L. B. Wu, H. Xiao, J. Wang, D. H. Lu, R. F. Zhou and R. Zhou, *Rare Metals*, 39(2015)214.
23. J. Qu, L. Y. Chen, Q. Meng, L. Z. Wu, X. P. Li, L. Q. Wang and W. J. Lü, *Mater. Mech. Eng.*, 40(2016)92.
24. B. Ye, Q. Ding, M. Qing, J. Zhou and H. J. Li, *J. Zhejiang Sci-Tech Univ.(Natural Sci.)*, 37(2017)502.
25. Y. Chen, X. H. Li, M. J. Fu and H. Ding, *J. Northeastern Univ.(Natural Sci.)*, 35(2014)1022.
26. S. H. Chen, L. Y. Jiang, C. L. Liu, W. J. Huang, Y. Y. Guo and Q. L. Xu, *Mater. Rev.*, 33(2019)1367.
27. Y. H. Jin, J. B. Zhao, C. F. Li and R. J. Huo, *J. Lanzhou Univ. Tech.*, 42(2016)27.
28. W. B. Xu, L. M. Ke and W. P. Xu, *Acta Mater. Compos. Sin.*, 28(2011)142.
29. D. Q. He, Y. Q. Sun, L. Ma and R. L. Lai, *Trans. China Weld. Inst.*, 39(2018)083.
30. W. Wang, K. S. Wang, J. L. Wu and W. L. Wang, *Ordance Mater. SCI. Eng.*, 31(2008)12.
31. C. B. Shen, Z. Z. Wang, G. F. Quan, S. H. Liu and J. P. Ge, *Corros. Sci. and Protection Tech.*, 22(2010)400.
32. C. L. Dong, J. H. Dong, H. X. Zhao, G. H. Luan and R. D. Fu, *Trans. China Weld. Inst.*, 33(2012)5.
33. W. L. Wang, W. Wang and W. Guo, *Hot Wor. Tech.*, 38(2009)8.
34. R. S. Mishra and Z. Y. Ma, *Mater. Sci. Eng. R*, 50(2005)1.
35. A. Squillace, A. De Fenzo, G. Giorleo and F. Bellucci. *J. Mater. Processing Tech.*, 152(2004)97.

© 2019 The Authors. Published by ESG (www.electrochemsci.org). This article is an open access article distributed under the terms and conditions of the Creative Commons Attribution license (<http://creativecommons.org/licenses/by/4.0/>).